RASĀYAN *J. Chem.*
Vol. 16 | No. 1 |261-267| January - March | 2023
ISSN: 0974-1496 | e-ISSN: 0976-0083 | CODEN: RJCABP
http://www.rasayanjournal.com
http://www.rasayanjournal.co.in

THE RECYCLING OF GRAPHITE FROM SPENT LITHIUM-ION BATTERIES AS NEW LITHIUM-ION BATTERIES ANODE MATERIALS

Y. L. Ni'mah[1,✉], S. Suprapto[1], C. A. Puteri[1] and A. Subhan[2]

[1]Chemistry Department, Faculty of Sciences and Data Analytics, Institut Technology Sepuluh Nopember, Surabaya 60111, Indonesia

[2]Research Center for Advanced Materials-National Research and Innovation Agency, Tangerang Selatan 15314, Indonesia

✉Corresponding Author: yatimnikmah@gmail.com

ABSTRACT

Spent lithium-ion batteries (LIBs) anode material has been successfully reused as a new LIBs anode material by mechanical separation, chemical purification, and calcination. The materials obtained were characterized using XRD and FTIR. LIBs anode slurry was made with a composition of active material: binder: additive = 85: 10: 5 that was mixed in N-methyl-2- pyrrolidone (NMP) solvents. Graphite of 5% was added to the anode active material to increase the graphite content in the anode materials. The battery performance was determined using cyclic voltammetry and the charge-discharge test. The charge-discharge test shows that the spent LIBs anode treated without the addition of graphite has the highest efficiency (98%) and capacity (charge 148.374 mAh/g and discharge 151.489 mAh/g). The capacity values were higher than the anode materials without treatment.

Keywords: Lithium-ion batteries, Anode materials, Graphite, LIBs recycle, NMP

RASĀYAN *J. Chem.*, Vol. 16, No.1, 2023

INTRODUCTION

The demand for electronic products such as cell phones, laptops, and tablets increases significantly year by year. Lithium-ion battery production increased from 2.05 billion units in 2005 to 5.86 billion units in 2012. It is predicted that the demand for LIBs increases by 25% each year.[1] The production of batteries, as a source of energy for portable electronic devices, also increased as a result of increasing consumer demand. Lithium-ion batteries (LIBs) are commonly used in portable electronic devices because of their lightweight and better storage capacity.[2] LIBs generally consist of an anode, cathode, separator, electrolyte, and outer protector. Commercial LIBs currently use various types of oxides and phosphates as cathode materials, such as $LiCoO_2$, $LiMn_2O_4$, $LiFePO_4$, $LiNi_{1-x-y}Co_xMn_yO_2$, and others.[3] The anode materials in most commercial LIBs were graphite. It is because of its capability and stability in storing lithium ions during charge-discharge cycles. Electrolytes that were often used in LIBs are lithium salts (such as $LiClO_4$, $LiNiO_2$, and $LiPF_6$) which were dissolved in organic solvents.[4] Spent LIBs was one of the sources of electronic waste. Boyden, 2016 stated that waste from electronic and electrical equipment is one of the fastest-growing types of waste, with the volume expected to increase by one-third times in 2013 (48.9 million tons) until 2017 (65.4 million tons). Increasing the amount of waste requires more land fields for disposal, and increases the number of hazardous chemicals which pollute the environment.[5] The amount of battery waste can be reduced by recycling the battery components that can be reused. The components of a lithium-ion battery can be separated mechanically or electrostatically. Several studies have been carried out to separate the metal component that can be reused in LIBs. Yuliusman, 2016, extracted lithium and cobalt metals using citric acid leaching. The leaching product purity was 98.08% for lithium and 86.28% for cobalt. Gao et. al. used sulfuric acid to remove metal ions from spent lithium-ion graphite.[6] Graphite as an anode material on lithium-ion batteries also has the potential to be recycled. Because the carbon composition in LIBs was 12–21% of the total composition of the LIBs.[7] Recycling graphite from spent LIBs anode material has several benefits, such as reducing electronic waste and providing a more economical source of graphite with good quality. Anode materials can be separated using mechanical separation from copper sheets and

http://doi.org/10.31788/RJC.2023.1618036

cathode materials. This research was focused on obtaining graphite material from spent LIBs anode using mechanical separation. The anode materials from spent LIBs were separated mechanically, then treated using a chemical solvent to remove the impurity such as binder and electrolytes from anode materials. The calcination was carried out to remove any residue from binders and solvents from graphite. Voltammetry and charge-discharge analysis of graphite recycled anode materials was carried out to observe the performance of the obtained anode materials.

EXPERIMENTAL

Material and Methods

The sample studied in this research was anode material obtained from spent NCR 18650 lithium-ion laptop batteries and new LIBs with similar types for comparison. The chemical used in this research i.e., KBr (Merck), Cu foil (TOB Machine), Li metal (LIPI Physics Workshop), N-methyl pyrrolidone 99.5% (NMP, Sigma Aldrich), Dimethyl carbonate 99% (DMC, Merck), Polyvinylidene fluoride (PVDF, Kynar Flex 28001-00), $LiPF_6$ (Lithium hexafluorophosphate), Graphite (LIPI Physics Workshop), Carbon black - Super P (Gellon), separator from TOB Machine, CR 2032 type coin cell series (TOB Machine), and acetone. The instrument used in this research i.e., XRD (X-Ray Powder Diffraction/ PANalytical Xpert MPD), Fourier Transform Infrared Spectrometer (FTIR/ Shimadzu 8400S), and potentiostat (WonAtech WBCS3000) for Cyclic Voltammetry and Charge-Discharge analysis. The battery copper sheet was removed from the spent LIBs to separate the anode material mechanically. The anode material was gently dredged using a metal blade. The same step was done for the new LIBs with the same type for comparison. The new anode materials were washed using DMC and NMP to remove the electrolytes and binder. The anode materials were then dried at 90°C.[8] The anode materials were calcined at 600°C using an N_2 atmosphere for 4 hours.[4] In this study, the variation of samples and the addition of fresh new graphite to the anode materials were carried out (Table-1).

Table-1: The Variation of Anode Materials

Sample Code	Type of Sample	Added Graphite
A01P	Used LIBs anode after treatment	0%
A51P	Used LIBs anode after treatment	5%
BFP	New LIBs anode after treatment	0%

Addition of 5% graphite was added to anode materials.[9-10] A gray powder was obtained after the calcination of the anode materials. The powder was ground using a pestle-mortar agate and sieved using 400 mesh screens. The addition of fresh graphite was done by mixing 3 g of the powder with 0.15 g of graphite. The LIBs slurry was prepared by dissolving 0.1176 g of PVDF as a binder with 1 mL of NMP. The mixture was heated at 70°C for 15 minutes and stirred for 15 minutes to dissolve PVDF. A carbon black of 0.0588 g was added to the mixture. The anode samples (A01P, A51P, and BFP) of 1 g each were mixed with the solution and stirred for 30 minutes. The solvent was added to obtain a slurry with suitable thickness. In this study the ratio of active material: binder: addictive material was 85: 10: 5.[11] The slurry was coated on copper foil using a doctor blade with a 200 μm thickness. The copper foil which has been coated with anode slurry was dried in a vacuum oven at 80°C and stored in an oven at 50°C.[10] The dried copper foil coated with anode slurry was cut in a disk shape, with a diameter of 16 mm. Commercial separators (19 mm) and Li metal were applied as cathodes (16 mm in diameter), LIBs half-cell. $LiPF_6$ as many as 3 drops were used as electrolytes in coin cells. The coin cell was assembled in a glove box with an argon gas flow. The coin cells were washed using acetone and allowed to stand until the voltage was stable. The coin cell was tested using cyclic voltammetry and the charge-discharge method.[12] The anode material of new and used LIBs was characterized using XRD to investigate their crystal structure. Both samples were measured with a radiation source of Cu Kα (λ = 1.5406Å), at a voltage of 40 kV and a current of 30 mA. The scan step used was 10.15 seconds at the angle of $5^o \leq 2\theta \leq 100^o$. FTIR characterization was carried out to compare the functional groups in new and spent LIBs anode materials before and after treatment. The FTIR measurement was carried out in the wavelength range of 4000-400 cm^{-1}. The samples were mixed with KBr in a ratio of 1: 99 using mortar agate. The mixture was pressed using hydraulic pumps to form a KBr disk. The KBr disk was placed in the FTIR sample holder and analyzed. Cyclic voltammetry was carried out to investigate the

oxidation-reduction current and potential of the lithium anode materials assembled into the lithium-ion battery coin cell. The cyclic voltammetry analysis was carried out using WonAtech WBCS3000 Automatic Battery Cycler with a scan rate of 0.1 mV/s in the voltage ranges from 0.0 V to 2.0 V (half-cell test). The capacity of the assembled lithium-ion battery coin cell was measured using a charge-discharged WonAtech WBCS3000 Automatic Battery Cycler instrument with a scan rate of 0.1 C in the voltage ranges from 0.0 V to 2.0 V (half-cell test). The performance of the battery can be observed from the capacity and efficiency as the function of loading current and electrode area. Battery efficiency was determined by comparing battery charging and discharge capacity.

RESULTS AND DISCUSSION

The anode materials from spent/used LIBs were mechanically separated and characterized using XRD. The anode materials from new LIBs were also characterized as a comparison. Both samples were measured with a radiation source of Cu Kα (λ = 1.5406Å), at a voltage of 40 kV and a current of 30 mA. The scan step used was 10.15 seconds with measuring angles of $5^o \leq 2\theta \leq 100^o$.

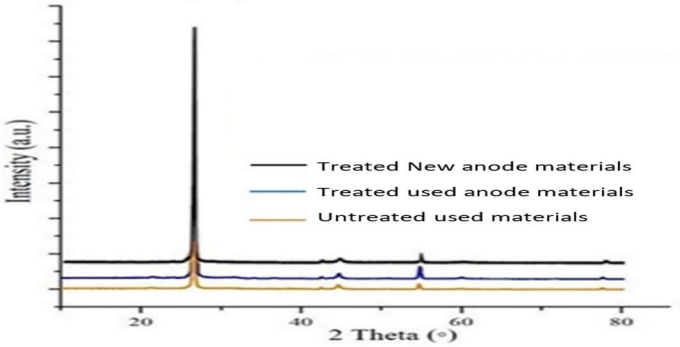

Fig.-1: XRD Diffractogram of New and used LIBs Anode Materials

The XRD diffractogram of the used and new LIBs anode material were shown in Fig.-1. Based on Fig.-1, there were no significant differences in both anode materials. The peaks that appear in both samples were at the same 2θ. The two anode materials show slight differences in their crystallinity. In the used LIBs anode materials, the crystallinity was lower than that of the new LIBs. This was indicated by the peak in the used LIBs which has a smaller intensity than the new LIBs. The anode materials in the new and used LIBs have a crystal structure that is compatible with JCPDS No. 96-901-1578. Thus, both anode materials have the same structure, which was a graphite structure. The anode materials from the used and new LIBs' mechanical separation were high-purity graphite. Missyul, *et al.,* 2017, explained that Li intercalation in graphite (Li_xC_6) can be identified by typical XRD diffractogram peaks as shown in Fig.-2(b). Pure graphite has a high peak at $26^o < 2\theta < 27^o$. This was consistent with the XRD characterization of the two anode materials presented in Fig.-2(a). Used LIBs anode material shows a high peak at $2\theta = 26.6^o$ and new LIBs at $2\theta = 26.7^o$. Thus, the LIBs anode materials structure did not change even though the battery has been used. Thus, the graphite in the anode material has the potential to be utilized again in the new LIBs.[13]

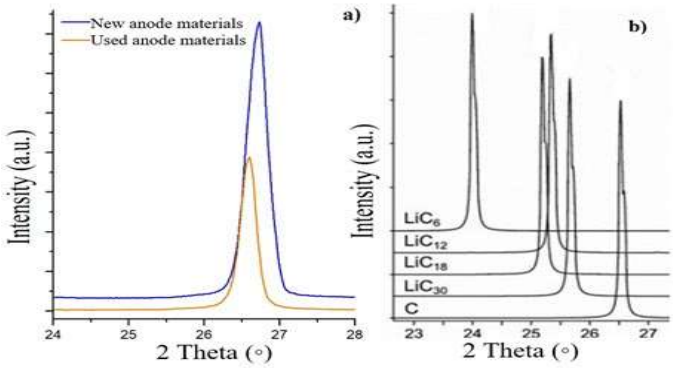

Fig.-2: (a) The XRD Diffractogram of New and Used LIBs Anode Materials, (b) XRD Diffractogram of Intercalated Li^+ Ions in the Graphite

The anode materials of used and new LIBs were characterized using FTIR to observe their functional groups. The FTIR spectra of new and used LIBs anode was shown in Fig.-3(a). The FTIR spectrum of anode material in both materials did not show any significant differences. Both materials generally have the same functional groups, as presented in Table-2.

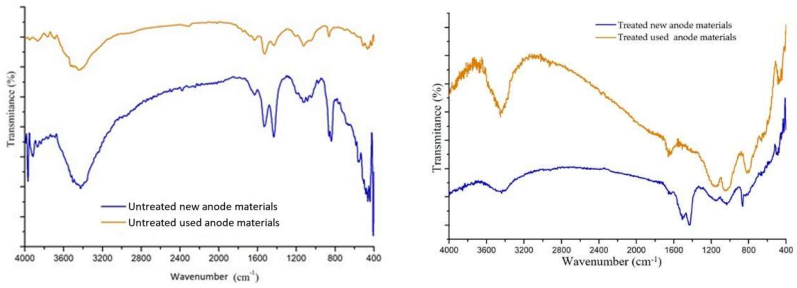

(a) (b)

Fig.-3: FTIR Spectra of (a) Untreated (b) Treated New and used LIBs Anode Materials

The FTIR spectrum in Fig.-3 indicates that the functional groups present in the used and new LIBs anode material were similar. Some impurities such as binders and electrolytes were present in the anode material and have to be removed. The binder residue in the used LIBs anode material covered the graphite surface so that it can inhibit the intercalation and de-intercalation of Li. This barrier can also decrease LIB's performance.

Table-2: FTIR Peaks of LIBs Anode Materials[14]

Functional Groups	Wavelength (cm^{-1})	
	New LIBs	Used LIBs
O-H	2900-3700	2900-3700
Ketone C=O)	1631.83	1629.90
C-F	1531.83 and1433.16	1529.60 and 1429.30
Amine (C-N)	1116.82	1126.47

The spent LIBs anode materials were washed using dimethyl carbonate (DMC) to remove the remaining electrolytes and NMP. The material was calcined at 600°C for 4 hours to vaporize the remaining solvent and remove the remaining impurities. The material obtained was characterized using FTIR to determine the effect of washing and calcination on the LIBs anode materials. Fig.-3 (b) shows the FTIR spectrum of the treated anode material and Table-3 summarizes the functional groups that were present in the materials. The treated LIBs anode material did not show any functional groups at wave number 1500-1400 cm^{-1}. This functional group comes from the C-F group derived from the PVDF binder. The FTIR spectrum of new LIBs anode materials that were only washed using DMC shows the presence of this C-F group. Thus, it was concluded that NMP was capable to dissolve the PVDF binder on the anode material. The FTIR spectra of both materials show the functional groups of C = O and C-N originating from solvent residue. The FTIR peak intensity of the treated materials was smaller than untreated materials. This indicates that washing and calcination were capable to reduce the presence of binders and other impurities in the anode materials.

Table-3: FTIR Spectra of LIBs-Treated Anode Materials[14]

Functional Groups	Wavelength (cm^{-1})	
	New LIBs	Used LIBs
O-H	3300-3700	3300-3700
Ketone C=O	1627.21	1656.14
Amine (C-N)	1151.34 and 1032.737	1168.22 and 1041.90
C-F	1428.57 and 1509.09	-

The anode material from used LIBs in the coin cell form was tested for their electrochemical characteristics by cyclic voltammetry and charge-discharge methods. The cyclic voltammogram gives information about the oxidation-reduction potential and current. The output of the charge-discharge test was the battery capacity. The CR 2032 coin cells consist of Li metal cathode (half-cell test) and graphite from the treatment of spent LIBs anode materials (Table-1), as well as $LiPF_6$ electrolyte. Coin cell was measured at a scan rate

of 0.1 mV/s at a potential of 0.0 – 2.0 V. All samples had a similar voltammogram as shown in Fig.-4. With varied peak current values (Table-4). LIBs coin cells from anode material without the addition of graphite (A01P) have an anodic peak current of 1.573 mA. This value was greater than LIBs from the new battery anode material with treatment (BFP), which was 1.074 mA. The sample with the highest peak current value, 2.771 mA, was obtained from the LIBs anode materials with the addition of 5% graphite (A51P).

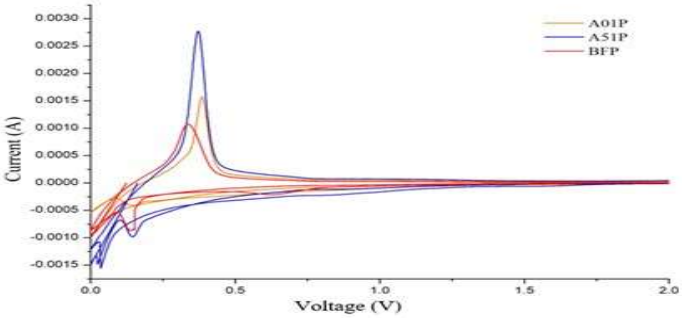

Fig.-4. LIBs cyclic Voltammogram of Treated Anode Materials

All samples have anodic potential in the range of 0.300 V (Table-4). The highest anodic potential was obtained from the A01P sample (0.386 V), while the lowest anodic potential was from the BFP sample (0.338 V). The A51P sample has an anodic potential value close to the anodic potential value of A01P (0.371 V). The anode material without treatment produces a high anodic potential, which was around 0.400 V, but the resulting anodic peak current was lower than LIBs that use treated anode materials. All treated anode material LIBs samples had an anodic peak current higher than those without treatment. The treated anode material (A01P) showed a higher peak current, 1.573 mA, compared to the anode material that was not treated, 0.156 mA. The addition of 5% graphite to the anode active material increases the peak current of LIBs. The LIBs consist of anode materials without treatment, the highest peak current of 0.315 mA was obtained from the AT51 sample, while in the anode materials with treatment, the highest peak current of 2.771 mA was obtained from the A51P sample. The cathodic peak current of the treated anode material appears in the potential of 0.150 V. A cathodic current of 0.409 mA was obtained from the A01P sample, 0.9842 mA from the A51P, and 0.7236 from BFP occur at a potential of 0.151 V; 0.145 V; and 0.138 V, respectively. The A51P sample has the highest cathodic and anodic peak current than the other samples, which proves that the addition of 5% graphite increases the peak current value of LIBs. The half-cell battery test shows that the treated anode material can be used as an anode material for LIBs.

Table-4: Anodic Peak Current of LIBs with Anode Material With and Without Treatment

Code	Sample	Graphite Addition	Peak Current (mA)	Potential (V)
AT01	Anode material from used LIBs without treatment	0%	0.156	0.454
AT51		5%	0.315	0.473
A01P	Anode material from used LIBs with treatment	0%	1.573	0.386
A51P		5%	2.771	0.371
BFP	Anode material from new LIBs	0%	1.074	0.338

The half potential ($E_{1/2}$) in a LIBs sample can be calculated using equation 1:

$$E_{1/2} = \frac{Epa - Epc}{2} \quad (1)$$

$E_{1/2}$ was half potential, Epa was oxidation peak potential and Epc was reduction peak potential. Using this equation, the average potentials obtained were 0.118 V for A01P, 0.113 V for A51P, and 0.100 V for BFP. The anode from used LIBs without the addition of graphite (A01P) has the highest average potential compared to the other samples. Thus, it was concluded that the anode material treated without the addition of fresh graphite, produces a better-applied potential than the anode material with the addition of fresh graphite and anode material from new LIBs. The charge-discharge test was carried out to determine the

battery capacity. Battery capacity describes the maximum amount of energy that can be released under certain conditions, expressed in mAh/g. The capacity value was equal to the number of lithium ions that transferred during a charge-discharge process. In the charging process, Li^+ undergoes intercalation into the anode material while in the discharge process, Li^+ undergoes de-intercalation from the anode materials into the cathode materials[15]. The weight of the tested materials can be seen in Table-5.

Table-5: The Composition of Anode Materials

Sample	Total Mass (g)	Mass of Cu foil (g)	Mass of Material (g)
A01P	0.0426	0.0277	0.0149
A51P	0.0485	0.0248	0.0237
BFP	0.0382	0.0265	0.0117

The treated anode material charge-discharge test was shown in Fig.-5. The capacity of each sample were shown in Table-6. The highest discharge capacity of 151.489 mAh/g was obtained from sample A01P and the highest charge capacity was 155.130 mAh/g obtained from sample A51P. The value of the used anode material capacity was higher than that obtained from the new anode material which produces a discharge capacity of 117.582 mAh/g and a charge of 111.693 mAh/g. A01P and BFP, have discharge capacity values that exceed the charge capacity. This was due to the presence of Li^+ ions that have been intercalated in the anode (graphite) active material before charging so that the Li^+ ions move along when discharges occur and produce a greater capacity than the charge capacity. Whereas in the A51P sample, the charge capacity was higher than the discharge capacity. This shows that Li was oxidized when it was charged, and not all of it was reduced back when discharged. This could be caused by the formation of a new SEI layer from the fresh graphite as a mixture in the treated anode materials.

Table-6: The Specific Capacity and Efficiency of the LIBs Sample

Code	Specific Capacity of Charge (mAh/g)	Specific Capacity of Discharge (mAh/g)	The efficiency of Charge/Discharge (%)
A01P	148.374	151.489	98
A51P	155.130	148.621	96
BFP	111.693	117.582	95

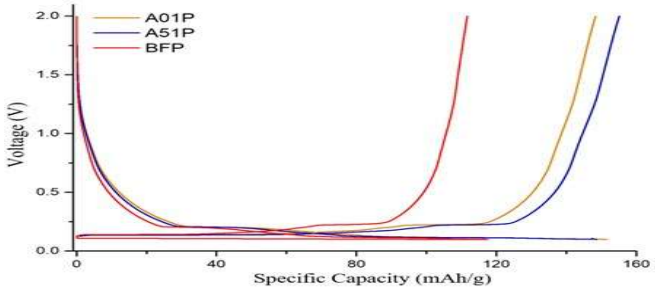

Fig.-5: The Charge-Discharge Curve of Treated Anode Materials

All the treated anode materials have charge-discharge efficiency that was close to 100%. The highest charge-discharge efficiency was obtained from an anode materials sample without the addition of graphite (A01P) whose efficiency reaches 98%. The lowest efficiency was 95% obtained from the new anode materials sample (BFP). The addition of graphite to the anode material decreases the charge-discharge efficiency. This could be due to incompatibility between fresh graphite and recycled graphite.

CONCLUSION

The anode material synthesized from spent LIBs has an average potential of 0.118 V which was higher than anode materials extracted from new LIBs anode (0.100 V). The addition of 5% graphite to the anode material increases the LIBs current to 2.771 mA but did not increase the applied potential. In the charge-discharge test, the highest efficiency (98%) was obtained from treated LIBs anode materials without the addition of graphite. The charge capacity value of 148.374 mAh/g and a discharge of 151.489 mAh/g were obtained.

ACKNOWLEDGMENTS

The authors gratefully acknowledge financial support from the Institut Teknologi Sepuluh Nopember for this work, under the project scheme of the Publication Writing and IPR Incentive Program (PPHKI) 2023.

CONFLICT OF INTERESTS

The authors declare that there is no conflict of interest.

AUTHOR CONTRIBUTIONS

All the authors contributed significantly to this manuscript, participated in reviewing/editing and approved the final draft for publication. The research profile of the authors can be verified from their ORCID ids, given below:

Y. L. Ni'mah https://orcid.org/0000-0002-5477-5544
S. Suprapto https://orcid.org/0000-0002-1490-0726
A. Subhan https://orcid.org/0000-0002-0774-9220

REFERENCES

1. L. Li, W. Qu, X. Zhang, J. Lu, R. Chen, F. Wu and K. Amine, *Journal of Power Sources*, **282**, 544(2015), https://doi.org/10.1016/j.jpowsour.2015.02.073
2. Y. L. Ni'mah, N. A. A. K. Hidayatullah, S. Suprapto, A. Subhan and A. Ardiansyah, *Moroccan Journal of Chemistry*, **10**(3), 396(2022), https://doi.org/10.48317/IMIST.PRSM/morjchem-v10i3.32667
3. B. Huang, Z. Pan, X. Su, and L. An, *Journal of Power Sources*, **399**, 274(2018), https://doi.org/10.1016/j.jpowsour.2018.07.116
4. B. Moradi and G. Botte, *Journal of Applied Electrochemistry*, **46**, 123(2016), https://doi.org/10.1007/s10800-015-0914-0
5. A. Boyden, V. K. Soo and M. Doolan, *Procedia CIRP*, **48**, 188(2016), https://doi.org/10.1016/j.procir.2016.03.100
6. Y. Gao, C. Wang, J. Zhang, Q. Jing, B. Ma, Y. Chen and W. Zhang, *ACS Sustainable Chemistry and Engineering*, **8**, 9447(2020), https://doi.org/10.1021/acssuschemeng.0c02321
7. L. Noerochim, W. Caesarendra, A. Habib, Widyastuti, Suwarno, Y. L. Ni'mah, A. Subhan, B. Prihandoko and B. Kosasih, *Energies*, **13**(20), 5251(2020), https://doi.org/10.3390/en13205251
8. H. F. Xiang, Z. D. Li, K. Xie, J. Z. Jiang, J. J. Chen, P. C. Lian, J. S. Wu, Y. Yud and H. H. Wang, *RSC Advances,* **2**(17), 6792(2012), https://doi.org/10.1039/C2RA20549A
9. Y. L. Ni'mah, M. F. Taufik, A. Maezah, and and F. Kurniawan, *Malaysian Journal of Fundamental and Applied Sciences*, **14**(4), 443(2018), https://doi.org/10.11113/mjfas.v14n4.970
10. C. Uthaisar, V. Barone, and B. Fahlman, *Carbon*, **61**, 558(2013), https://doi.org/10.1016/j.carbon.2013.05.037
11. B. Setiawan, V. Iasha, and U. Hikmah, *International Journal of Scientific & Technology Research*, **9**(6), 737(2020)
12. C. R. Birkl, E. McTurk M. R. Roberts, P. G. Bruce, and D. A. Howey, *Journal of The Electrochemical Society*, **162**(12), A2271(2015)
13. A. Missyul, I. Bolshakov, and R. Shpanchenko, *Powder Diffraction*, **32**, 1(2017), https://doi.org/10.1017/S0885715617000458
14. D. Pavia, G. Lampman, G. Kriz, and J. Vyvyan, *Introduction to spectroscopy*. Harcourt College Publishers, (2015).
15. V. J. Ovejas and A. Cuadras, *Scientific Report*, **9(1)**, 14875(2019), https://doi.org/10.1038/s41598-019-51474-5

[RJC-8036/2022]